http://ansinet.com/itj



ISSN 1812-5638

INFORMATION TECHNOLOGY JOURNAL



Asian Network for Scientific Information 308 Lasani Town, Sargodha Road, Faisalabad - Pakistan

Application of Improved Sparse A* Algorithm in UAV Path Planning

^{1,2}Miao Yong-Fei, ¹Zhong Luo and ²Xia Luo-Sheng
 ¹School of Computer Science and Technology, Wuhan University of Technology,
 Wuhan, Hubei 430070, China
 ²Dalian Air Force Sergeant School of Communication, Dalian, Liaoning, 116600, China

Abstract: It's necessary to study in Unmanned Aerial Vehicle (UAV) three-dimensional path planning and smoothing method in real digital terrain environment because of shortcomings existing. At present, mathematical simulation is often adapted to generate the terrain during the process of the UAV flight path planning, which lacks the reality of performing tasks. Aimed at this case, this study has proposed an Improved Sparse A* Algorithm (ISAA) that introducing the real digital terrain after interpolation and curvature smoothing into planning space. The algorithm combines the terrain constraints and the kinetics constraints of the UAV in the search process of the A * algorithm. And, cubic cardinal spline curves are adapted to smooth the generated three-dimensional path and this makes the path can meet the demands of the curvature and torsion of the UAV. Finally, Experiment results show that this algorithm has reduced the search space and increased the convergence speed. In addition, final planning path is feasible.

Key words: Digital terrain, UAV, A* algorithm, path planning, curve smoothing

INTRODUCTION

Nowadays frequent natural disasters in our country often occur with serious damages of surface transportation facilities. It's becoming a serious problem that how to quickly and effectively get the news about the situation of the disaster areas and personnel casualties and set up the air rescue network security system of disaster accidents. The UAV has advantages of cheap cost, flexibility, high reliability and no need to worry about extra personnel casualties. Thus, it's widely used at the scene of the earthquake relief, mountain rescue and other emergency search and rescue (Almurib et al., 2011). Path planning of the UAV is the key component of the UAV mission planning. It means to plan out feasible flight path which meets a variety of constraint conditions (Yang et al., 2012). Many scholars home and abroad have put forward different solutions about path planning problems of the UAV.

Hao and Xin (2010) has smoothed DEM date generated by simulation to the surface of minimum risk. To improve generic algorithm's weakness of easily being trapped into local optimum, it introduces metropolis criterion of simulated annealing algorithm. Lastly, it obtains better paths and accelerates the convergence speed. But in that case topographic data may be unreal and the flight path cannot meet the demands of the

curvature and torsion of the UAV. Khuswendi et al. (2011) puts forward A* three dimensional planning algorithm based on artificial potential field theory and receding horizon. This algorithm has achieved a good result because it makes up the shortcoming that artificial potential field method is easily trapped into local optimum point and the convergence speed of A* algorithm is slow. On the other hand, this algorithm also has some shortcomings of simple model construction and low feasibility of flight path. Liu et al. (2013) mixes ant colony optimization with cultural algorithm. It redesigns population space and belief space of cultural ant colony algorithm and solves the three-dimensional flight path which meets the requirement of time and space. This algorithm has accelerated the convergence speed of flight planning, but still not smoothed the flight path after planning.

During the process of flight planning, various problems arise. For example, the terrain lacks the reality, the convergence speed is slow, it's easily being trapped into the local optimal solution and the flight planning cannot meet the dynamic constraints of the UVA. Aimed at these problems, this study presents an Improved Sparse A* Algorithm (ISAA) of path planning on the basis of real digital terrain. It adapts cubic cardinal spline curve to smooth the generated path and this makes the paths can meet the demands of the dynamic constraints of the UVA.

MODELING OF PLANNING SPACE

Before flight planning, flight environment and related factors in flight planning (mainly are terrain, meteorological condition, etc.,) should be represented as symbol information for the purpose of computer processing. Given the mission objectives of the UAV the study studies, planning space mainly includes digital terrain information and weather information.

Digital terrain and interpolation: The digital elevation modal in this study is SRTM (Shuttle Radar Topography Mission). Data acquisition method is airborne radar scanning acquisition. The organizational form of SRTM data is to divide the file into a number of grid umits and each file corresponds to a tile of 1x1 degree. According to the sampling interval, the data can be divided into SRTM-1 and SRTM-3 and each respectively corresponds with sampling intervals 1 and 2 arc seconds. The terrain data used in simulation comes from SRTM-3 of International Data Mirroring Sites of Computer Network Information Center, Chinese Academy of Science (CAS), raw data of digital elevation is 90 m resolution.

For the raster data model of DEM only gives elevation information of the sampling points and uses the elevation value of them to approximately represent the elevation of the whole raster unit. Obviously, the higher the resolution of DEM, the better representation of the terrain. While SRTM-3 resolution cannot meet the demands of actual flight, terrain data needs interpolation and smoothing. In this study, bilinear interpolation method is adapted to interpolate terrain data. The principle of bilinear interpolation is shown in Fig. 1.

The elevation of E will be calculated like Eq. 1:

$$Z_{e} = Z_{e} (\Delta \overline{x} \Delta \overline{y} - \Delta \overline{x} - \Delta \overline{y} + 1) + Z_{b} (-\Delta \overline{x} \Delta \overline{y} + \Delta \overline{x}) + Z_{c} (-\Delta \overline{x} \Delta \overline{y} + \Delta \overline{y}) + Z_{c} (\Delta \overline{x} \Delta \overline{y} + \Delta \overline{y}) + Z_{c} (\Delta \overline{x} \Delta \overline{y} + \Delta \overline{y}) + Z_{c} (\Delta \overline{x} \Delta \overline{y} + \Delta \overline{y}) + Z_{c} (\Delta \overline{x} \Delta \overline{y} + \Delta \overline{y}) + Z_{c} (\Delta \overline{x} \Delta \overline{y} + \Delta \overline{y}) + Z_{c} (\Delta \overline{x} \Delta \overline{y} + \Delta \overline{y}) + Z_{c} (\Delta \overline{x} \Delta \overline{y} + \Delta \overline{y}) + Z_{c} (\Delta \overline{x} \Delta \overline{y} + \Delta \overline{y}) + Z_{c} (\Delta \overline{x} \Delta \overline{y} + \Delta \overline{y}) + Z_{c} (\Delta \overline{x} \Delta \overline{y} + \Delta \overline{y}) + Z_{c} (\Delta \overline{x} \Delta \overline{y} + \Delta \overline{y}) + Z_{c} (\Delta \overline{x} \Delta \overline{y} + \Delta \overline{y}) + Z_{c} (\Delta \overline{x} \Delta \overline{y} + \Delta \overline{y}) + Z_{c} (\Delta \overline{x} \Delta \overline{y} + \Delta \overline{y}) + Z_{c} (\Delta \overline{x} \Delta \overline{y} + \Delta \overline{y}) + Z_{c} (\Delta \overline{x} \Delta \overline{y} + \Delta \overline{y}) + Z_{c} (\Delta \overline{x} \Delta \overline{y} + \Delta \overline{y}) + Z_{c} (\Delta \overline{x} \Delta \overline{y} + \Delta \overline{y}) + Z_{c} (\Delta \overline{x} \Delta \overline{y} + \Delta \overline{y}) + Z_{c} (\Delta \overline{x} \Delta \overline{y} + \Delta \overline{y}) + Z_{c} (\Delta \overline{x} \Delta \overline{y} + \Delta \overline{y}) + Z_{c} (\Delta \overline{x} \Delta \overline{y} + \Delta \overline{y}) + Z_{c} (\Delta \overline{x} \Delta \overline{y} + \Delta \overline{y}) + Z_{c} (\Delta \overline{x} \Delta \overline{y} + \Delta \overline{y}) + Z_{c} (\Delta \overline{x} \Delta \overline{y} + \Delta \overline{y}) + Z_{c} (\Delta \overline{x} \Delta \overline{y} + \Delta \overline{y}) + Z_{c} (\Delta \overline{x} \Delta \overline{y} + \Delta \overline{y}) + Z_{c} (\Delta \overline{x} \Delta \overline{y} + \Delta \overline{y}) + Z_{c} (\Delta \overline{x} \Delta \overline{y} + \Delta \overline{y}) + Z_{c} (\Delta \overline{x} \Delta \overline{y} + \Delta \overline{y}) + Z_{c} (\Delta \overline{x} \Delta \overline{y} + \Delta \overline{y}) + Z_{c} (\Delta \overline{x} \Delta \overline{y} + \Delta \overline{y}) + Z_{c} (\Delta \overline{x} \Delta \overline{y} + \Delta \overline{y}) + Z_{c} (\Delta \overline{x} \Delta \overline{y} + \Delta \overline{y}) + Z_{c} (\Delta \overline{x} \Delta \overline{y} + \Delta \overline{y}) + Z_{c} (\Delta \overline{x} \Delta \overline{y} + \Delta \overline{y}) + Z_{c} (\Delta \overline{x} \Delta \overline{y} + \Delta \overline{y}) + Z_{c} (\Delta \overline{x} \Delta \overline{y} + \Delta \overline{y}) + Z_{c} (\Delta \overline{x} \Delta \overline{y} + \Delta \overline{y}) + Z_{c} (\Delta \overline{x} \Delta \overline{y} + \Delta \overline{y}) + Z_{c} (\Delta \overline{x} \Delta \overline{y} + \Delta \overline{y}) + Z_{c} (\Delta \overline{x} \Delta \overline{y} + \Delta \overline{y}) + Z_{c} (\Delta \overline{x} \Delta \overline{y} + \Delta \overline{y}) + Z_{c} (\Delta \overline{x} \Delta \overline{y} + \Delta \overline{y}) + Z_{c} (\Delta \overline{x} \Delta \overline{y} + \Delta \overline{y}) + Z_{c} (\Delta \overline{x} \Delta \overline{y} + \Delta \overline{y}) + Z_{c} (\Delta \overline{x} \Delta \overline{y} + \Delta \overline{y}) + Z_{c} (\Delta \overline{x} \Delta \overline{y} + \Delta \overline{y}) + Z_{c} (\Delta \overline{x} \Delta \overline{y} + \Delta \overline{y}) + Z_{c} (\Delta \overline{x} \Delta \overline{y} + \Delta \overline{y}) + Z_{c} (\Delta \overline{x} \Delta \overline{y} + \Delta \overline{y}) + Z_{c} (\Delta \overline{x} \Delta \overline{y} + \Delta \overline{y}) + Z_{c} (\Delta \overline{x} \Delta \overline{y} + \Delta \overline{y}) + Z_{c} (\Delta \overline{x} \Delta \overline{y} + \Delta \overline{y}) + Z_{c} (\Delta \overline{x} \Delta \overline{y} + \Delta \overline{y}) + Z_{c} (\Delta \overline{x} \Delta \overline{y} + \Delta \overline{y}) + Z_{c} (\Delta \overline{x} \Delta \overline{y} + \Delta \overline{y}) + Z_{c} (\Delta \overline{x} \Delta \overline{y} + \Delta \overline{y}) + Z_{c} (\Delta$$

And:

$$\Delta \mathbf{x} = (\mathbf{x}_e - \mathbf{x}_a)/1$$
$$\Delta \mathbf{y} = (\mathbf{y}_e - \mathbf{y}_a)/1$$

The digital terrain after bilinear interpolation is shown in Fig. 2:

Construction of weather model: During the flight of the UAV, those weather types which have a significant impact upon the safety and performance of the UAV are usually sandstorm, thunderstorm, hail, severe convection, strong breeze and so on (Ceccarelli *et al.*, 2007). However, the weather changes little between the heights of the

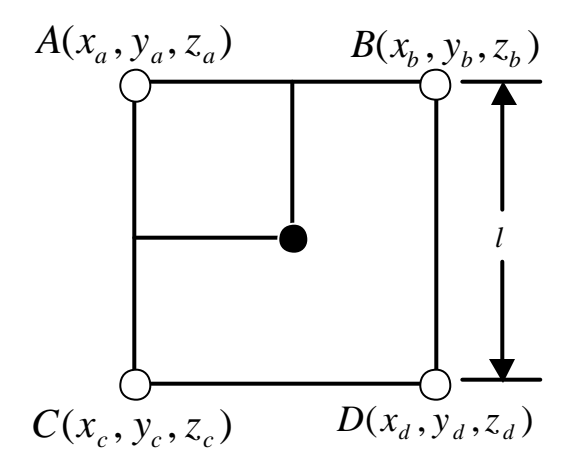


Fig. 1: Bilinear interpolation

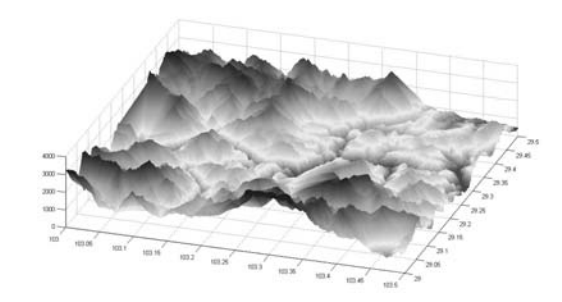


Fig. 2: Digital terrain

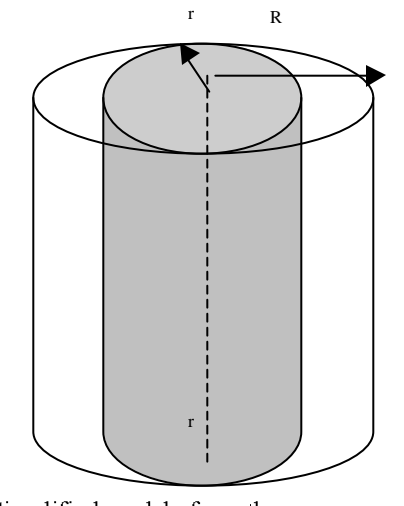


Fig. 3: Simplified model of weather

maximum pitching angle range of the UAV. Therefore, as shown in Fig. 3, the cylinder is used to approximately simulate the impact area of bad weather (Zhang *et al.*, 2007).

In order to simplify the model, the influence of meteorological threatened area on the UAV can be considered uniformly distributed. So, the probability density function can be expressed as follows:

$$W = \begin{cases} 1, d \le r \\ \frac{d-r}{R-r}, r < d < R \\ 0, d \ge R \end{cases}$$
 (2)

Hereinto, d is the distance from the node to the center of bad weather and r stands for the radius of the center of bad weather and R is the maximum influence distance of bad weather.

PATH PLANNING AND SOMOOTHING

Basic principles of sparse A* algorithm: As the heuristic search algorithm, A* algorithm is one of the most classic method of the application of the flight planning of the UAV. A* algorithm often represents planning space in grid form and seeks the optimal path through preconcerted cost function. It calculates the cost of each grid unit that can be reached and then adds the unit with the lowest cost into searching space. Those units in the searching space can be used to produce more possible paths. The cost function A* algorithm adapts is shown as follows:

$$f(x) = g(x) + h(x)$$
(3)

Here g(x) represents the real cost from initial position to current node. h(x) is heuristic function and it represents the estimated value of the cost from current node to target node. During the iteration of A^* algorithm, it always chooses the node with the lowest f(x) value and interpolate it into possible path chain list. It's proved that as long as h(x) is less than or equal to the real cost from current code to target node, which means that it meets acceptable conditions and feasible solution exists, then A^* algorithm is able to find the optimal solution.

Szczerba et al. (2000) proposes an improved A* algorithm named sparse A* algorithm. This algorithm adds the constraint condition to the searching process of the algorithm, which effectively trims useless nodes in planning space and greatly shorten the search time. However, in a practical application, long search time is still the bottleneck that restricts sparse A* algorithm because of too large planning space and complex constraint conditions (Meng and Gao, 2010).

Principles of ISAA: The basis of path planning algorithm is the rasterization of planning space. Logical division ways can establish far more practical solving space. This study utilizes the constraint condition of the UAV to decompose three-dimensional planning space and further extends sparse A* algorithm to the three-dimensional space.

Table 1: Data structure of OPEN list

State Coordinate of Coordinate of Fitness of indication current node parent node current node

0/1 x y z X Y Z g h f

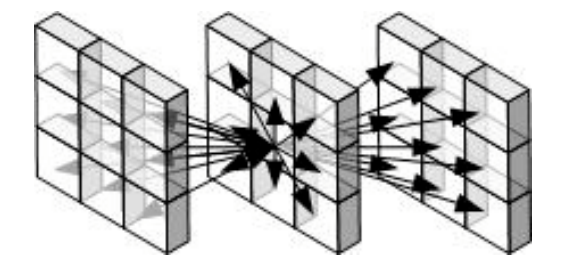


Fig. 4: Searching nodes before clipping

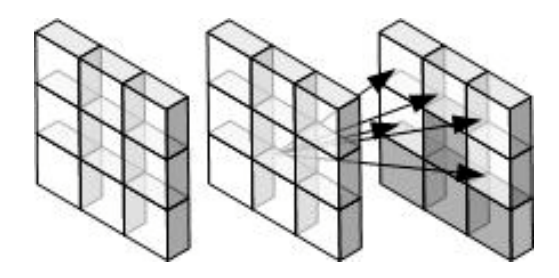


Fig. 5: Searching nodes after clipping

The criterion of the horizontal subdivision is to satisfy the constraints of the minimum step length and the maximum turning angle of the UAV. The size of the grid is the minimum step length of the UAV. With the minimum step length 1 km and the maximum turning angle 45°, for example, the space should be divided into 1km×1km. Then the next feasible node generated on the basis of the previous horizontal heading contains at most three grid units. Similarly, we should divide the vertical according to the maximum climbing/diving angle. In order to improve the accuracy, the grid size in horizontal and vertical can be further subdivided to increase expanding nodes.

To reduce the seek for useless nodes (For example, the center zone of airflow, no-fly zone and nodes under the terrain) during solving process, useless nodes should be written into the CLOSE list during initialization. It can reduce feasible nodes during the expanding process of OPEN list and accelerate the convergence speed of the algorithm. The data storage of OPEN list is shown in Table 1.

Figure 4 and 5 show the searching nodes which are comprehensively considered about dynamics constraint and useless nodes before and after. It shows that there are 26 searching nodes before clipping, the number drops to 9 when considering dynamics constraint and it becomes 5 after considering about useless nodes (4 useless nodes).

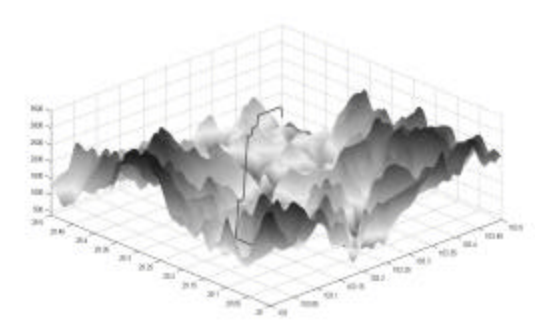


Fig. 6: Planning path by ISAA

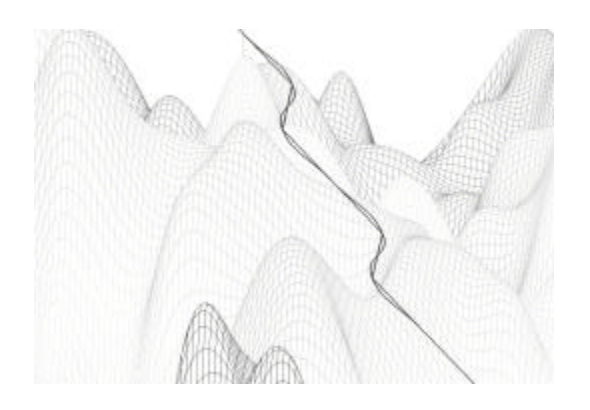


Fig. 7: Path smoothing by cubic cardinal spline curve

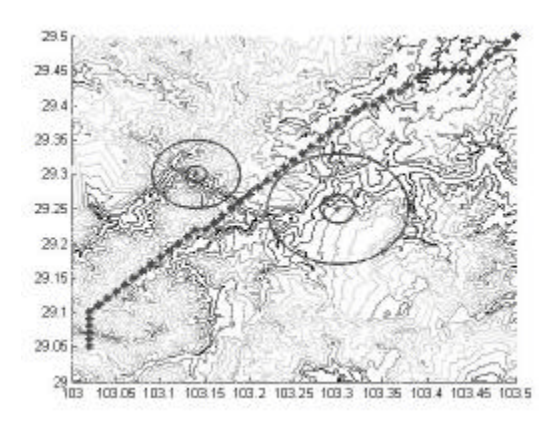


Fig. 8: View in contour map

After establishing the rasterization space of A^* algorithm, it's time to design the cost function of A^* algorithm. Real cost is divided as distance cost g(x), climbing cost d(x) and weather threat cost t(x). Then, g(x) can be expressed as follows:

$$g(x) = k_1 * d(x) + k_2 * c(x) + k_3 * t(x)$$
(4)

Here, k_1 , k_2 , k_3 are cost weighting factors and it satisfies the equation:

$$\sum_{i=1}^{3} k_i = 1$$

Heuristic function h(x) is the Euclidean distance between current point and target point. Figure 6 shows the result path planned by ISAA.

Cubic cardinal spline curves: Cardinal spline curves interpolate piecewise cubic with specified endpoint tangents for each segment. But there is no need for Cardinal splines to give the tangent value of the endpoint (Yang and Sukkarieh, 2008) For Cardinal splines, the slope of a control point can be calculated through the coordinates of two contiguous control points.

One Cardinal spline can be determined by four continuous control points. Among them, the two control points in the middle are the endpoints of the curve segment and the other two points are used to calculate the end slope of the curve section.

Set four continuous control points as $P_{k\cdot l}$, $P_{k\cdot l}$, $P_{k\cdot l}$, $P_{k\cdot l}$, $P_{k\cdot l}$, and set P (u) as parameter cubic function (u means parameter), Between control points P_k and $P_{k\cdot l}$. Then the boundary conditions that the four points $P_{k\cdot l}$ to $P_{k\cdot l}$ are used to set up Cardinal splines are as follows:

$$P(0) = P_{k}$$

$$P(1) = P_{k+1}$$

$$P'(0) = (1 - t) * (P_{k+1} - P_{k-1})$$

$$P'(1) = (1 - t) * (P_{k+2} - P_{k})$$
(5)

In other words, the slopes of the control points P_k and P_{k+1} are, respectively proportional to those of the chords $P_{k+1},\,P_{k\cdot l}$ and $P_{k+2},\,P_k.$

Parameter t is the tension coefficient. For t controls the tightness degree between the Cardinal spline and input control point, Solve the four equations above and transform it into matrix form as follows.

$$P(\mathbf{u}) = \left[\mathbf{u}^3 \, \mathbf{u}^2 \, \mathbf{u} \, \mathbf{1}\right] \bullet \mathbf{M}_c \bullet \begin{bmatrix} \mathbf{P}_{k-1} \\ \mathbf{P}_k \\ \mathbf{P}_{k+1} \\ \mathbf{P}_{k-2} \end{bmatrix}$$
(6)

Matrix Cardinal is as follows:

$$\mathbf{M}_{c} = \begin{bmatrix} -\mathbf{s} & 2 - \mathbf{s} & \mathbf{s} - 2 & \mathbf{s} \\ 2\mathbf{s} & \mathbf{s} - 3 & 3 - 2\mathbf{s} - \mathbf{s} \\ -\mathbf{s} & 0 & \mathbf{s} & 0 \\ 0 & 1 & 0 & 0 \end{bmatrix}$$
 (7)

And s = 1-t/2

Finally, the pseudo code of ISAA can be realized as Table 2.

Table 2: Pseudo code of ISAA

Pseudo code of ISAA

Read DEM,OPEN = [], CLOSE = [useless nodes]

While (All nodes state indication aren't 0)

Choose the node x with smallest fitness cost value

If (x=Target node)

Break; Else

For(child nodes of x)

Generate feasible nodes set by comparing with CLOSE list. Then write them in OPEN list.

End for

End if

Insert x into CLOSE list, Chang the state indication of x from 1 to 0. End while

Optimal path smoothing and printing

Table 3: Simulation data

Algorithm	Convergence time (s)	Cost function	Optimal path (km)
A* algorithm	6.325	35.67	147.93
ISAA	3.128	28.16	134.78

EXPERIMENT RESULTS AND ANALYSIS

The ISAA in this study is realized in Matlab platform. It adapts the digital terrain of 50×50 km and the coordinates are 103°~103°30′E longitude and 29°~29°30′N latitude. The coordinates of the center of bad weather are (103°18′E, 29°15′N) and (103°6′E, 29°18′N). The former's radius of the center zone is 1000 m and the maximum distance is 4000 m. And those of the latter are 600 and 2500 m.

The simulation result has verified that the flight path planned by this algorithm was very close to the digital terrain and grids with low cost function were chosen as the evolution direction. Table 3 explained the fact that since the algorithm added useless nodes into CLOSE list, searching nodes were reduced and convergence time was accelerated. And cost function and distance of the optimal flight path got by using this improved algorithm were much less than those by using traditional A* algorithm.

CONCLUSION

The ISAA put forward in this study applied real digital terrain after interpolating to the flight planning of the UAV, which made planning space more close to actual demand. Moreover, it clipped useless nodes in searching space and so shortened searching time and accelerated convergence speed. The algorithm made use of cubic spline to smooth generated flight path and made the resulting flight path far more practical with application prospects.

ACKNOWLEDGMENTS

The authors would like to thank for the support by National Natural Science Foundation of China under the

Grant 61003130 and Grant 61303029. The authors also thanks for the support by Wuhan Technology Department Innovation Project (2013070204005).

REFERENCES

- Almurib, H.A.F., P.T.Nathan and T.N. Kumar, 2011. Control and path planning of quadrotor aerial vehicles for search and rescue. Proceedings of the SICE Annual Conference, September 13-18, 2011, Tokyo, Japan, pp: 700-705.
- Hao, M. and G.Z. Xin, 2010. UAV route planning based on the genetic simulated annealing algorithm. Proceedings of the IEEE International Conference on Mechatronics and Automation, August 4-7, 2010, IEEE, Xi'an, China, pp. 788-793.
- Liu, Z.F., H.S. Xie and S.G. Wei, 2013. Aircraft 3-D route planning based on culture-ant algorithm. Comput. Simul., 30: 99-103.
- Meng, B.B. and X.G. Gao, 2010. UAV path planning based on bidirectional sparse a search algorithm.
 Proceedings of the International Conference on Intelligent Computation Technology and Automation, Volume 3, May 11-12, 2010, IEEE Computer Society, Changsha, pp. 1106-1109.
- Ceccarelli, N., J.J. Enright, E. Frazzoli, S.J. Rasmussen and C.J. Schumacher, 2007. Micro UAV path planning for reconnaissance in wind. Proceedings of the American Control Conference, July 9-13, 2007, IEEE, New York, USA., pp: 5310-5315.
- Szczerba, R.J., P. Galkowski, I.S. Glicktein and N. Ternullo, 2000. Robust algorithm for real-time route planning. IEEE Trans. Aerospace Electr. Syst., 36: 869-878.
- Khuswendi, T., H. Hindersah and W. Adiprawita, 2011. UAV path planning using potential field and modified receding horizon a 3D algorithm. Proceedings of the International Conference on Electrical Engineering and Informatics, July 17-19, 2011, IEEE, Bandung Indonesia, pp. 1-6.
- Yang, F., Y. Zhuang and J.Z. Xiao, 2012. 3D PRM based real-time path planning for UAV in complex environment. Proceedings of the IEEE International on Robotics and Biomimetics, December 11-14, 2012, IEEE, Guangzhou, China, pp. 1135-1140.
- Yang, K.J. and S. Sukkarieh, 2008. 3D smooth path planning for a UAV in cluttered natural environments. Proceedings of the IEEE/RSJ International Conference on Intelligent Robots and Systems, September 22-26, 2008, IEEE, Nice, France, pp: 794-800.
- Zhang, Y., J. Chen and L.C. Shen, 2007. Military aircraft route planning based on probabilistic map. Comput. Simul., 24: 62-66.